Egyptian Journal of Chemistry

Synthesis of 3-Dimensional Chitosan/Carboxymethyl Cellulose/ZnO Biopolymer Hybrids by Ionotropic Gelation for Application in Drug Delivery

Marwa M. Metwally,[a,b]* Rafael Muñoz-Espí,[b] Ibrahim Youssef,[a] Doria S. Badawy,[a] Magdy Y. Abdelaal[a]

[a]. Chemistry Department, Faculty of Science, Mansoura University, Mansoura, ET-35516-Egypt,

[b]. Institute of Materials Science (ICMUV) Universitat de València C/ Catedràtic José Beltrán 2, Paterna 46980, Spain

Abstract

Chitosan (CS) and carboxymethyl cellulose (CMC), as ecofriendly biopolymers, were self-assembled to form a 3-dimensional network and a hybrid material with ZnO nanoparticles (ZnO-CMC/CaCl₂/CS). The designed system was used as a carrier for *in-vitro* release of 5-fluorouracil drug. The drug loading capacity and entrapment efficiency were investigated. Swelling behavior of the prepared systems and the cumulative release of the drug were studied at different concentrations of the raw materials at pH values of 2.1 and 7.4, which was emulated to the human gastrointestinal medium. The release kinetic data were fitted using the Korsmeyer-Peppas model to identify the diffusion mechanism. The prepared copolymers were characterized by Fourier transform infrared (FTIR) spectroscopy, thermogravimetric analysis (TGA) and scanning electron microscopy (SEM).

1. Introduction

The synthetic anionic modified cellulose which is known as carboxymethyl cellulose (CMC) is formed by carboxymethylation of cellulose. CMC possesses eco-friendly properties, such as safety, biodegradability, biocompatibility, non-toxicity, and sensitivity to different environments. Also the availability of CMC, would qualify it to enter easily the pharmaceutical, clinical and food industries [1-3]. Presence of anionic carboxylate group (COO⁻) enables CMC to have electrostatic interactions with ionic salts to form microspheres with Al^{3+}, Fe^{3+} or Ca^{2+} by ionotropic gelation. The anionic COO⁻ group also allow the polyelectrolytic CMC chains to interact with other oppositely charged polyelectrolytes (e.g., chitosan) to form a 3-dimensional polyelectrolyte complex hydrogel network. Covalent cross-linking can be achieved in the presence of citric acid or glutaraldehyde to form hemiacetal [4-7].

Chitosan is a natural cationic polymer produced by deacetylation of chitin extracted from shrimp peel. Chitosan is a natural polysaccharide containing an amino group and can dissolve in a diluted solution of acetic acid as a result of protonation of amino group forming NH_3^+ cationic group [8-11]. The protonated amino groups allow the formation of chitosan beads by ionic gelation through the interaction with negatively charged ionic salts, such as sodium tripolyphosphate (TPP). It may also result in a polyelectrolyte complexation with negatively charged polymers, such as sodium alginate, CMC or carboxymethyl chitosan. Such ionic interactions are described as physical cross-linking. Chemical cross-linking may be produced by dialdehydes (e.g., glutaraldehyde), forming Schiff bases through the covalent bond formation. This reaction may produce copolymerization with oxidized polysaccharides [12-16]. Chitosan is an eco-friendly polymer similar to CMC.

Addition of inorganic zinc oxide nanoparticles (ZnO NPs) to polymers is promising since it has a brilliant activity in different applications. ZnO NPs are characterized by their photo physical properties, non-toxicity, safety toward the human body (FDA code 182.8991 [17, 18]) and availability. The entrapment of ZnO NPs into polymers, leads to a change in the polymeric geometrical structure, which

can be used for drug delivery applications. In addition the swelling properties of the polymer can be enhanced, which would improve the cumulative release percentage [19-21].

The current study introduces an example of fabricated self-assembled ZnO-CMC/CaCl$_2$/CS bio-nanocomposite hydrogels. The introduced pH-sensitive biopolymer was ionically crosslinked with CaCl$_2$ to be used as a carrier for 5-fluorouracil release.

2. Experimental:
2.1. Materials

High molecular weight chitosan (CS) was acquired from Sigma Aldrich; sodium salt of carboxymethyl cellulose (Na-CMC) (average M.W. 250000, DS = 0.7), 1-pentanole, 5-flourouracil (5-FU) and *m*-xylene were purchased from Acros Organics; calcium chloride anhydrous, zinc acetate and *p*-toluene sulfonic acid monohydrate were purchased from Sigma Aldrich; glacial acetic acid was acquired from Panreac-Química.

2.2. Synthesis of ZnO NPs by wet-chemical method

ZnO NPs were synthesized by wet-chemical method, as reported by Demir et al. [22]. 2.5 g of zinc acetate, as a zinc precursor, was added to a mixture of 52 mmol *p*-toluene sulfonic acid monohydrate, which was dissolved firstly in 25 mL of *m*-xylene and 50 mL of 1-pentanol. The reaction mixture was refluxed for 2 h in oil bath at 130 °C. Afterward, the NPs were collected by centrifugation for 10 min at 4000 rpm. The separated NPs were dried under vacuum at 40°C and preserved for further use. A small amount of ZnO NPs was redispersed in ethanol (1mg/mL) under sonication and diluted for dynamic light scattering (DLS) measurements (Zetasizer Nano ZS, Malvern Instruments). The average size of the ZnO NPs was 34±3 nm.

2.3. Formation of hybrid ZnO/CMC/CS hydrogel

1g of CMC was dissolved in 100 mL distilled water under magnetic stirring for 3 h until complete dissolution. The hydrophilic drug (5-FU) was dissolved in a little amount of water and then added to the CMC solution (0.5 mg/mL) under continuous stirring. ZnO NPs were well dispersed in distilled water under sonication and added to the CMC/5-FU mixture at a rate of 0.5g/mL. The mixture was continuously stirred for further 2 h. The ionic cross-

linker CaCl$_2$ (5%) was added to the system (ZnO/CMC/5-FU), leading to entrapping the drug and the ZnO NPs into the CMC network. The cross-linked ZnO-CMC-drug suspension was added dropwise using a syringe pump at a rate of 1 mL/min into chitosan solution (1 g dissolved in 2% (v/v %) acetic acid solution) as shown in Table (1). The addition was done under stirring to avoid agglomeration. The self-assembly of the two polymers is shown in Graph (1) and (2).
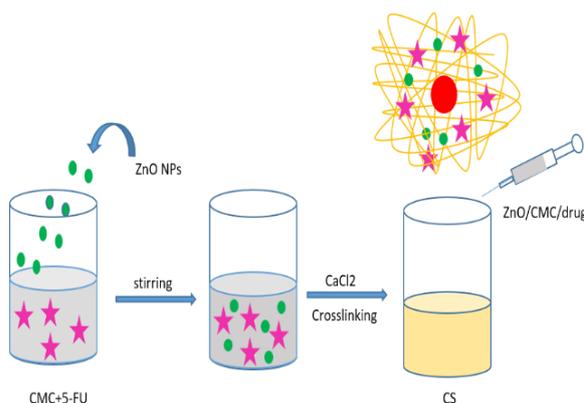
Graph (1): Preparation of ZnO-CMC-CaCl$_2$/CS hybrids by ionotropic gelation

Table 1: Composition of the biopolymers and ZnO NPs

Sample	S1	S2	S3	S4	S5	S6
CMC:CS	1:1	3:1	1:3	1:1	1:1	1:1
ZnO-NPs (%)	2.1	2.1	2.1	–	1.04	4.2
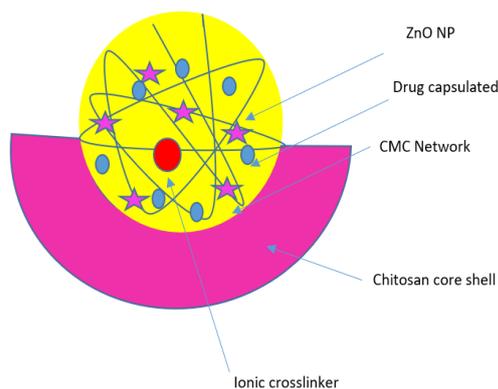
Graph (2): Schematic representation of the self-assembly cross-linking

2.4. Evaluation of encapsulation efficiency (EE %) and loading capacity (LC %)

For evaluating the entrapment efficiency (EE %), the circular-shaped particles of ZnO/CMC/CaCl$_2$/CS were separated from the liquid system by filtration.

The filtrate was diluted as needed for UV-vis spectroscopy measurements (SECOMAM UVI Light UV-Visible Spectroscopy) at 266 nm (λ_{max} of 5-FU). For determination of the loading capacity (1.6 wt. %), a dry amount of the nanocomposite was dissolved in phosphate buffer solution (pH 7.4), and the polymer was dissolved/suspended for 10 min under sonication. Afterward, the sample was filtered, and the amount of drug released was measured by UV-vis spectroscopy. The following equations Eq. (1) and Eq. (2) were used for the calculations:

Encapsulation Efficiency (EE%) =

$$= \frac{\text{Actual amount of 5-FU in nanocomposites}}{\text{intial amount of 5-FU}} \times 100$$

Eq. (1)

Loading capacity (LC%) =

$$\frac{\text{total amount of 5-FU} - \text{free 5-FU in supernatant}}{\text{nanocomposite yield}} \times 100 \quad \text{Eq. (2)}$$

2.5. Further characterization

Attenuated total reflectance Fourier transform infrared (ATR-FTIR) spectra were recorded on an ATR Agilent Cary 630 spectrometer. Measurements were conducted from 4000 to 400 cm^{-1} at room temperature. Thermogravimetric analysis (TGA) was carried out by heating the samples from 27 to over 900 °C under N$_2$ atmosphere with a heating rate of 10 °C/min in a TGA-50 thermobalance (TA Instruments). Scanning electronic micrographs were taken in a Hitachi S4 800 scanning electron microscope (SEM) at am acceleration voltage of 5 kV after coating the samples by a thin layer of platinum as a conducting surface.

2.6. Equilibrium swelling behavior

Equilibrium swelling behavior of the bio-nanocomposites was achieved by measuring the difference in weight through the time after absorbing the medium solution at pH = 2.1 and pH = 7.4 by immersing the sample into the different buffer solutions for 8 h. The swelling ratio was calculated from Eq. (3),

Swelling Ratio% $= \frac{m_t - m_o}{m_o} \times 100$ Eq. (3)

Where m_t is the mass of the swollen sample at time t and m_0 is the initial sample mass.

The swelling/deswelling process was performed by successive swelling and drying the samples for three times to ensure that the samples reached nearly

constant weight, reflecting that the weight loss of the samples due to repeating the process is negligible. The whole weight loss of the samples after swelling/deswelling cycles was only 1−2%.

2.7. 5-FU Cumulative release study.

The *in-vitro* cumulative release of 5-FU was measured by immersing a weighed part of the hydrogel samples ($\approx$ 0.1g) into 30 mL of the buffer medium (pH 2.1 and pH 7.4, which are similar to pH in gastrointestinal environment at 37°C). A known volume of the buffer solutions was added in the quartz cuvette and the corresponding UV-vis spectrum was recorded. The amount of drug released was calculated by the aid of a calibration curve of the drug, calculating the CDR % from Eq. (4) and (5):

$$\text{CDR\%} = \frac{\text{amount of drug released in medium}}{\text{amount of loaded druginto the hydrogel}} \times 100$$

Eq. (4)

$Amount\ of\ drug(mg/l) =$

$$\frac{\text{concentration} \times \text{dil.factor} \times \text{vol.of dissolution medium}}{1000} \quad \text{Eq. (5)}$$

2.8. 5-FU release kinetics

In this work, the kinetic release data of 5-FU was fitted to a Korsmeyer-peppas model [24], expressed by Eq. (4):

$$\frac{M_t}{M_i} = Kt^n \qquad \text{Eq. (4)}$$

Where Mt is the amount of drug released at time t, M_i is the initial amount of drug in the system, the fraction M_t/M_i is the drug release (%) at time t, K is the Korsmeyer constant for release rate and n is the drug diffusion exponent. For studying the kinetics of 5-FU release according to Korsmeyer-Peppas, the logarithmic cumulative 5-FU release log (M_n/M_i) was plotted vs. log time (log t). The value of n was determined from the slope of this linear relationship. The value of the diffusion exponent, n, indicates the diffusion mechanism. With $n<0.5$, $0.5<n<1.0$, $n=1.0$ or $n>1.0$, the drug release mechanism may obey Fickian diffusion, anomalous transport, case-II transport (polymer erosion) or super case-II transport, respectively.

3. Results and Discussion
3.1. Fourier Transfer Infrared spectroscopy (FTIR)

The FTIR spectrum of chitosan showed a broad peak at 3300 cm^{-1} which is corresponding to the

presence of both OH and NH$_2$ groups overlapped at this range (Fig. (1)). The peaks at 1640 and 1562 cm^{-1} belong to the stretching frequency of amides I and II [25]. The peaks observed at 1300–1400 cm^{-1} and 1000–1100 cm^{-1} are attributed to the stretching frequency of C–N and C–O, in the polysaccharide skeleton respectively. the broad peak observed at 3370 cm^{-1} in the CMC spectrum ascribed to the stretching bending of OH groups interlayers. The characterized peaks at 1645 cm^{-1}, 1420 cm^{-1} were shifted to 1582 cm^{-1} and 1005 cm^{-1}, which could be attributed to the vibration bending of OH of the uronic acid structure[26, 27]. For the spectrum of ZnO-CMC/CaCl$_2$/CS, the obviouse reduction in peak intensity at 3370 cm^{-1} could be related to the electrostatic interaction between COO$^-$ and NH$_2$ in CMC and CS, respectively. The shift in the peak at 1617 cm^{-1} was attributed to the ionic force between Ca^{2+} and COO$^-$ The physical cross-linking and presence of chitosan in the matrix could be explained by the shift observed at 3382 cm^{-1}.
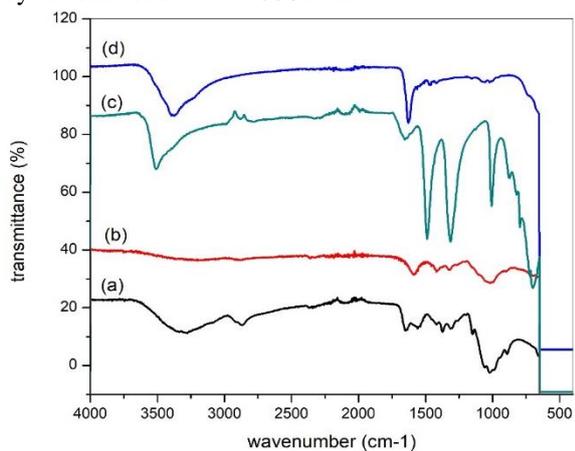
Figure (1): FTIR spectrum for (a) pristine chitosan, (b) pristine CMC and (c) CS/ZnO-CMC/CaCl$_2$

3.2. Thermogravimetric analysis (TGA)

Thermogravimetric analysis was carried out for pristine chitosan, Na-CMC and ZnO-CMC/CaCl$_2$/CS. The corresponding thermograms are shown in Fig. (2). The thermal degradation of the polymers and copolymer was mainly achieved in three stages. The loss weight about 10% was corresponded to the removal of the moisture content at 80–250 °C. The 50% rapid weight loss at 280–400°C, which is ascribed to the decomposition of the polymer and the elimination of volatile components. The residual parts were about 40% ZnO and 10-13% Na$_2$O in ZnO-CMC/CaCl$_2$/CS and pristine Na-CMC,

respectively, [28]. There was no residual in case of pristine chitosan, since the whole sample was degraded to water and CO$_2$.
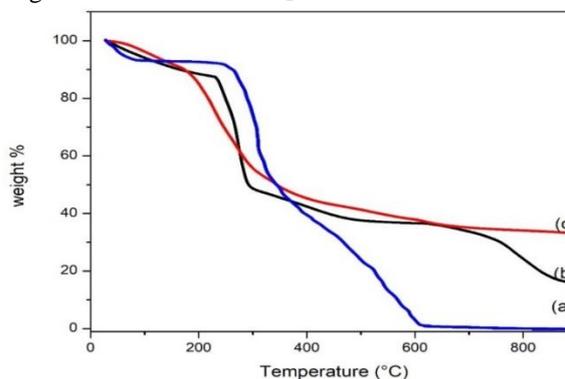
Figure (2): TGA of a) native chitosan, b) native Na-CMC and c) CS/ZnO-CMC/CaCl$_2$

3.2. Evaluation of the encapsulation efficiency (EE %) and the loading capacity (LC %)

The drug encapsulation efficiency (EE %) is a potential parameter for promoting the polymer matrix for drug delivery applications. Low drug loading values may cause drug wasting, which makes the matrix economically less convenient for the human treatment. As shown in Fig. (3), polymers and ZnO NPs contents have an effect on the encapsulation efficiency, since the loading efficiency of ZnO-CMC/CaCl$_2$/CS was fluctuating between 27.9% and 50.5. The highest encapsulation efficiency was obtained for sample S4 (without ZnO NPs). The EE% decreased by increasing the concentration of ZnO NPs [29, 30]. The values obtained were 27.95%, 37.23%, 45.47% and 50.28% for samples S6, S1, S5, and S4, respectively. This can be a consequence of the crusty and rough surface of the ZnO/CMC polymer hybrid. The complex surface reduced the dripping of 5-FU inside the polymer. Increasing in CMC content in samples S1–S3 lead to an increase in the 5-FU entrapment, which ranged from 30.5% to 41.9%. CMC contains COO$^-$ groups that interact with phenolic and amino groups present in 5-FU, which increases the absorbance of the drug. On the other hand, chitosan enhanced the entrapment of the drug due to the attractive interaction between NH$_3^+$ and phenolic OH$^-$ groups of the drug, however, the further increase in chitosan content decreased in the encapsulation efficiency. This may be attributed to the rough nature of the chitosan shell formed, that surrounded the Zn/CMC/CaCl$_2$ matrix, which in turn might be inhibiting the leakage of the drug within the network.
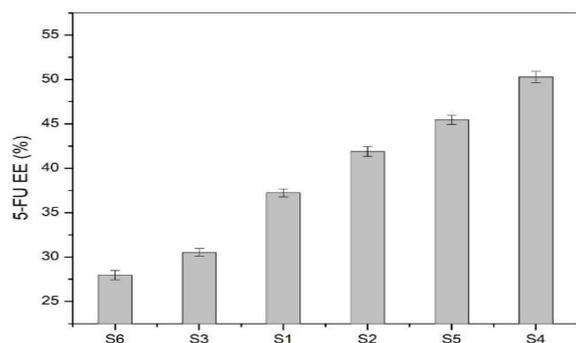
Figure (3): 5-FU entrapment efficiency of CS/ZnO-CMC/CaCl$_2$ samples S1–S6

3.3. Scanning electronic microscopy (SEM)

SEM images of hybrid sample (S5) demonstrated a smooth morphology with slight protrusions on the surface shown (Fig. (4)). It may confirm the physical cross-linking of CMC with CaCl$_2$ followed by the physical cross-linking with the chitosan and forming a shell. Higher magnifications indicated the presence of rough aggregates which was ascribabled to the presence of ZnO NPs.
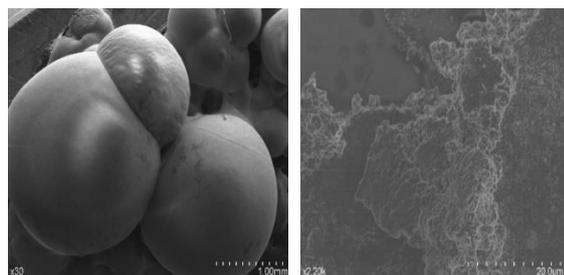
Figure (4): SEM images of ZnO-CMC/CaCl$_2$/CS (S5)

3.3. Swelling studies

Swelling ratios for CS/ZnO-CMC/CaCl$_2$ copolymer samples were studied at 37 °C at pH 2.1 and 7.4 for 8 h. The results presented in Fig. (5) indicate that the swelling equilibrium trend was generally increased at pH 7.4. This may be due to the ionic cross-linking of CMC with chitosan, which dissolved in slightly alkaline and neutral medium, and the ion exchange of Ca^{2+} ions and phosphate ions in phosphate buffer solution. A variation in the maximum swelling ratios was found for samples S1–S6, as the contents of CMC, CS and ZnO NPs were varied. At pH 2.1, the maximum swelling ratios were 356.6%, 275.7%, 402.6%, 319.1%, 428.3%, and 407.24%; and at pH 7.4, the maximum swelling ratios were 752.6%, 812.3%, 558.8%, 668.4%, 841.2% and 778.1%, for samples S1 to S6, respectively. The samples at pH 7.4 had a high swelling and shrinkage ability, with nearly complete solubility at neutral medium.

Fig. (5a) studies the effect of CS and CMC content on the swelling behaviour. Increasing the content of CMC leads to an increase in the swelling ratio at pH 7.4 due to the deprotonation of free carboxylic groups and ion exchange of Ca ions with phosphate ions from the medium, causing an increase of the osmotic pressure. An increase of the chitosan content causes an increase in the swelling ratio at pH 2.1, as a result of the solubility of chitosan in acidic media. At pH 7.4, the slightly alkaline medium causes the deprotonation of chitosan (NH$_3^+$ groups deprotonate to NH$_2$), which causes precipitation of chitosan [31,32].
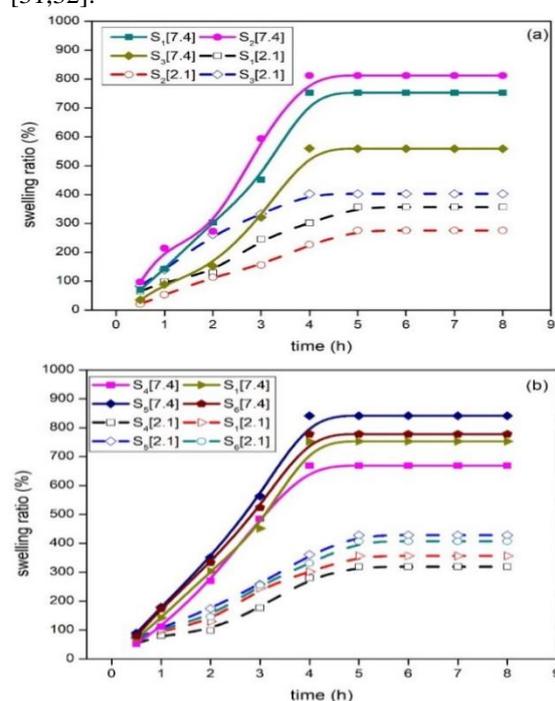
Figure (5): Swelling behavior of CS/ZnO-CMC/CaCl$_2$ samples at pH 2.1 and 7.4 (a) Effect of polymer content for samples S1-S3, and (b) Effect of ZnO NPs content for samples S1and S4-S6.

Fig. (5b) illustrates the effect of the ZnO NPs content on the swelling ratio. By increasing ZnO NPs, the swelling ratio increases until a limit and then it decreases slightly. ZnO NPs cause difference in the sizes of the polymeric matrix, leading to an increase of pores that allow penetration of the medium solution inside the polymeric network. ZnO NPs occupy different spaces in the polymeric matrix, after expansion of the matrix by swelling water, which helps the NPs to release out of the matrix, leaving free spaces that absorb more water amounts.

3.4. *In-vitro* drug release study

Cumulative 5-FU release from the copolymer network CS/ZnO-CMC/CaCl$_2$/5-FU was studied at pH 2.1 and 7.4 at 37°C within 12 h. The results are shown in Fig. (6).

There is a direct relationship between the swelling ratio and the cumulative drug release, as the shrinkage of water inside the polymeric network causes extension of the chains [33, 34]. Furthermore, the presence of pores allows the exit of the drug. At the early stage, there was an initial fast release until 4 h; after that, the release rate became slower until stability. Increasing CMC, CS and ZnO NPs causes variation of the cumulative drug release, depending on pH value. The maximum CDR% was about 84% for S5 at pH 7.4, when the contents of CMC and ZnO NPs were the highest. Increasing CMC causes also an increase in the swelling ratio and, subsequently, an increase in the drug release. Generally, CS/ZnO-CMC/CaCl$_2$ bio nanocomposite may act as a good carrier for release of 5-FU drug in the human gastrointestinal tract.

3.4. 5-FU release kinetics

The 5-FU cumulative release data were fitted with a Korsmeyer-Peppas model for studying its kinetic mechanism, as shown in Fig. (7). The various diffusion indexes (n) for samples S1-S6 at pH 2.1 and pH 7.4 are presented in Table (2). The results indicate n values around 0.5 at pH 2.1 and around 0.3 at pH 7.4, which confirms that the kinetic mechanism of this hydrogel mainly undergoes a Fickian diffusion [35, 36].
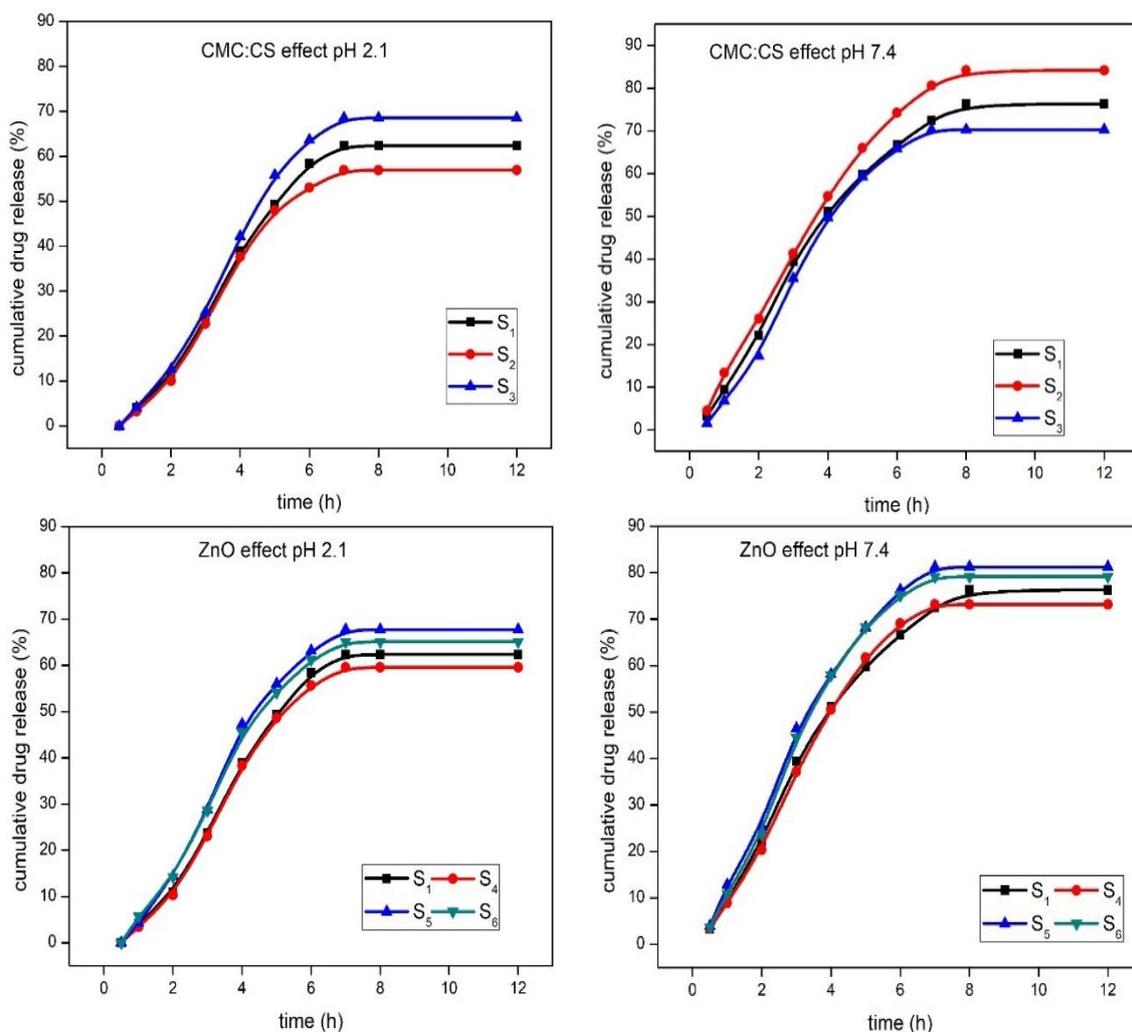
Figure (6): Cumulative release of 5-FU at pH 2.1 and pH 7.4 for samples S1-S7.
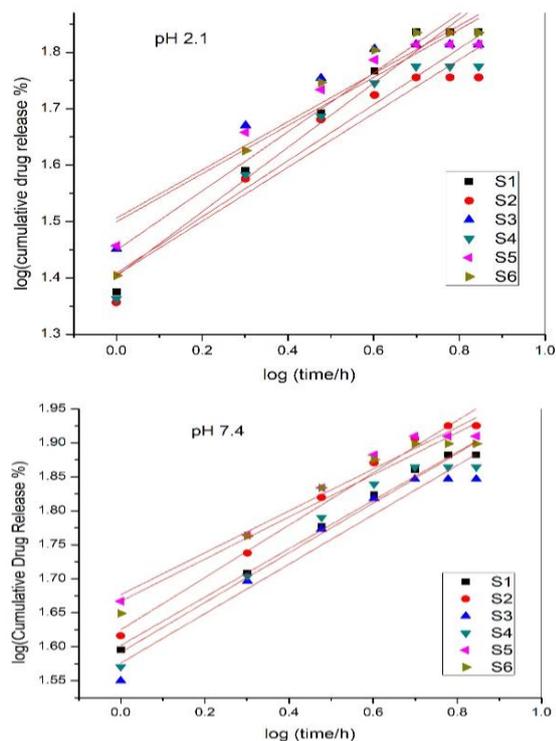
Figure (7): kinetic release of 5-FU from samples S1-S6 according to Korsmeyer-Peppas model at pH 2.1 and pH 7.4.

Table 2: Correlation coefficient (R^2) and Release exponent (n) according to Korsmeyer- Peppas model for samples S1-S7 at (a) pH 2.1 and (b) pH 7.4

	pH 2.1		pH 7.4	
Sample code	Release exponent (*n*)	correlation coefficient (R^2)	Release exponent (*n*)	correlation coefficient (R^2)
S1	0.5692	0.9634	0.3556	0.9886
S2	0.4775	0.9093	0.3851	0.9823
S3	0.4269	0.9014	0.3637	0.9405
S4	0.4974	0.9196	0.3657	0.9429
S5	0.4266	0.9158	0.3081	0.9600
S6	0.5237	0.9208	0.3102	0.9461

4- Conclusion

CMC/ZnO hybrid nanoparticles were physically cross-linked with CaCl$_2$ through electrostatic interaction and ionic gelation. The crosslinking was followed by the ionic complexation with chitosan to form a self-assembled polymeric network as an *in-vitro* pH-sensitive hydrogel carrier for 5-fluorouracil. The investigation proved that the maximum release achieved for ZnO/CMC/CaCl$_2$/CS hydrogel was 84% at pH 7.4. The copolymer network showed very reproducible swelling/deswelling processes. The raw materials used in the manufacturing procedure are safe, green, economic, biodegradable and biocompatible. More studies are undergoing in order to enhance the drug cumulative release.

5. References

1. Wang, M., Jia X., Liu W. and Lin X., *Water insoluble and flexible transparent film based on carboxymethyl cellulose.* Carbohydrate Polymers, 2021. **255**: 117353.
2. Cai, Y., Lihua H., Xia T., Jiaqi S., Bifen C., Feibai Z., Mouming Z., Qiangzhong Z., and Paul Van der Meeren, *Effect of pH on okara protein-carboxymethyl cellulose interactions in aqueous solution and at oil-water interface.* Food Hydrocolloids, 2021. **113**: 106529.
3. Sun, X., Chao L., Omer A.M., Wuhuan L., Shuxing Z., Xun J., Hongjie W., Di Y. and Xiao-kun O., *pH-sensitive ZnO/carboxymethyl cellulose/chitosan bio-nanocomposite beads for colon-specific release of 5-fluorouracil.* International journal of biological macromolecules, 2019. **128**: 468-479.
4. Hosseini-Aghdam, S.J., Foroughi-Nia, B., Zare-Akbari, Z., Mojarad-Jabali, S., motasadizadeh, H. and Farhadnejad, H., *Facile fabrication and characterization of a novel oral pH-sensitive drug delivery system based on CMC hydrogel and HNT-AT nanohybrid.* International journal of biological macromolecules, 2018. **107**: 2436-2449.
5. Lotfy, V.F. and Basta A.H., *Optimizing the chitosan-cellulose based drug delivery system for controlling the ciprofloxacin release versus organic/inorganic crosslinker, characterization and kinetic study.* International Journal of Biological Macromolecules, 2020. **165**:1496-1506.
6. Rao, Z., Hongyu G., Liangling L., Chen Z., Lian M., Meng L., Lihong F., and Dan L., *Carboxymethyl cellulose modified graphene oxide as pH-sensitive drug delivery system.* International journal of biological macromolecules, 2018. **107**:1184-1192.

7. Wang, H., Zichao L., Samia Y., Hassan H., Moaaz K. Seliem, Adrian Bonilla-P., Guilherme L. D., Lotfi S., and Qun L, *Effective adsorption of dyes on an activated carbon prepared from carboxymethyl cellulose: Experiments, characterization and advanced modelling.* Chemical Engineering Journal, 2021. **417**: 128116.

8. Abdelghany, A.M., Menazea A.A., and Ismail A.M., *Synthesis, characterization and antimicrobial activity of Chitosan/Polyvinyl Alcohol blend doped with Hibiscus Sabdariffa L. extract.* Journal of Molecular Structure, 2019. **1197**: 603-609.

9. Abdelaal, M. Y., Abdel-Razik E.A., Abdel-Bary E.M., El-Sherbiny I.M., *Chitosan-based interpolymeric pH-responsive hydrogels for in vitro drug release.* Journal of applied polymer science, 2007. **103**(5): 2864-2874.

10. Moramkar, N. and Bhatt P., *Insight into chitosan derived nanotherapeutics for anticancer drug delivery and imaging.* European Polymer Journal, 2021.**154**: 110540.

11. Iqbal, O., Shahid S., Ghulam A., Akhtar R., Muhammad H., Mehran A., and Zunaira A., *Moxifloxacin loaded nanoparticles of disulfide bridged thiolated chitosan-eudragit RS100 for controlled drug delivery.* International Journal of Biological Macromolecules, 2021. **182**: 730-742.

12. Dev, A., Binulal N.S., Anitha A., Nair S.V., Furuike T., Tamura H., Jayakumar R., *Preparation of poly (lactic acid)/chitosan nanoparticles for anti-HIV drug delivery applications.* Carbohydrate polymers, 2010. **80**(3): 833-838.

13. Wu, Z., Jun S., Pingan S., Jingguo L., and Shaokui C., *Chitosan/hyaluronic acid based hollow microcapsules equipped with MXene/gold nanorods for synergistically enhanced near infrared responsive drug delivery.* International Journal of Biological Macromolecules, 2021. **183**: 870-879.

14. Affes, S., Inmaculada A., Niuris A., Ángeles H., Moncef N., and Hana M., *Chitosan derivatives-based films as pH-sensitive drug delivery systems with enhanced antioxidant and antibacterial properties.* International Journal of Biological Macromolecules, 2021. **182**: 730-742.

15. Bernkop-Schnürch, A. and Dünnhaupt S., *Chitosan-based drug delivery systems.* European journal of pharmaceutics and biopharmaceutics, 2012. **81**(3): 463-469.

16. Nagpal, K., Singh S.K., and Mishra D.N., *Chitosan nanoparticles: a promising system in novel drug delivery.* Chemical and Pharmaceutical Bulletin, 2010. **58**(11): 1423-1430.

17. Jebel, F.S. and Almasi H., *Morphological, physical, antimicrobial and release properties of ZnO nanoparticles-loaded bacterial cellulose films.* Carbohydrate polymers, 2016. **149**: 8-19.

18. Huang, X., Zheng X., Xu Z., and Yi C., *ZnO-based nanocarriers for drug delivery application: From passive to smart strategies.* International journal of pharmaceutics, 2017. **534**(1-2):190-194.

19. Yadollahi, M., Farhoudian S. S., Barkhordari S., Gholamali I., Farhadnejad H., Motasadizadeh H. *Facile synthesis of chitosan/ZnO bio-nanocomposite hydrogel beads as drug delivery systems.* International journal of biological macromolecules, 2016. **82**: 273-278.

20. Singh, T.A., Das J., and. Sil P.C, *Zinc oxide nanoparticles: A comprehensive review on its synthesis, anticancer and drug delivery applications as well as health risks.* Advances in Colloid and Interface Science, 2020: 102317.

21. Sadhukhan, P., Kundu M., Chatterjee, S., Ghosh N., Manna P., Das J. and Sil P. C., *Targeted delivery of quercetin via pH-responsive zinc oxide nanoparticles for breast cancer therapy.* Materials science and engineering: C, 2019. **100**: 129-140.

22. Demir, M.M., Muñoz-Espí R., Lieberwirth I. and Wegner G., *Precipitation of monodisperse ZnO nanocrystals via acid-catalyzed esterification of zinc acetate.* Journal of Materials Chemistry, 2006. **16**(28): 2940-2947.

23. Tan, L.S., Tan H.L., Deekonda K., Wong Y.Y., Muniyandy S., Hashim K. and Pushpamalar J., *Fabrication of radiation cross-linked diclofenac sodium loaded carboxymethyl sago pulp/chitosan hydrogel for enteric and sustained drug delivery.* Carbohydrate Polymer Technologies and Applications, 2021. **2**: 100084.

24. Peppas, N., *Analysis of Fickian and non-Fickian drug release from polymers.* Pharmaceutica Acta Helvetiae, 1985. **60**(4): 110-111.

25. Papadimitriou, S., Bikiaris D., Avgoustakis K., Karavas E. and Georgarakis M., *Chitosan nanoparticles loaded with dorzolamide and pramipexole.* Carbohydrate polymers, 2008. **73**(1): 44-54.

26. Su, J.-F., Huang Z., Yuan X.-Y., Wang X.-Y. and Li, M., *Structure and properties of carboxymethyl cellulose/soy protein isolate blend edible films crosslinked by Maillard reactions.* Carbohydrate polymers, 2010. **79**(1): 145-153.

27. Asnag, G., Oraby A., and Abdelghany A.M., *Green synthesis of gold nanoparticles and its effect on the optical, thermal and electrical properties of carboxymethyl cellulose.* Composites Part B: Engineering, 2019. **172**: 436-446.

28. Neto, C.d.T., Giacometti J.A., Job A.E., Ferreira F.C., Fonseca J.L.C. and Pereira M.R., *Thermal analysis of chitosan based networks.* Carbohydrate Polymers, 2005. **62**(2): 97-103.

29. Hua, S., Yang H., Wang W. and Wang, A., *Controlled release of ofloxacin from chitosan–montmorillonite hydrogel.* Applied Clay Science, 2010. **50**(1): 112-117.

30. Upadhyaya, L., Singh J., Agarwal V., Pandey A. C., Verma S. P., Das P. and Tewari R. P., *In situ grafted nanostructured ZnO/carboxymethyl cellulose nanocomposites for efficient delivery of curcumin to cancer.* Journal of Polymer research, 2014. **21**(9): 1-9.

31. George, D., Maheswari P.U., and Begum K.M.S., *Chitosan-cellulose hydrogel conjugated with L-histidine and zinc oxide nanoparticles for sustained drug delivery: Kinetics and in-vitro biological studies.* Carbohydrate polymers, 2020. **236**: 116101.

32. George, D., Maheswari P.U., and Begum K.M.S., *Synergic formulation of onion peel quercetin loaded chitosan-cellulose hydrogel with green zinc oxide nanoparticles towards controlled release, biocompatibility, antimicrobial and anticancer activity.* International journal of biological macromolecules, 2019. **132**: 784-794.

33. Barkhordari, S., Yadollahi M., and Namazi H., *pH sensitive nanocomposite hydrogel beads based on carboxymethyl cellulose/layered double hydroxide as drug delivery systems.* Journal of Polymer Research, 2014. **21**(6): 1-9.

34. Zare-Akbari, Z., Farhadnejad H., Furughi-Nia, B., Abedin S., Yadollahi M. and Khorsand-Ghayeni M., *PH-sensitive bionanocomposite hydrogel beads based on carboxymethyl cellulose/ZnO nanoparticle as drug carrier.* International journal of biological macromolecules, 2016. **93**: 1317-1327.

35. Costa, P. and Lobo J.M.S., *Modeling and comparison of dissolution profiles.* European journal of pharmaceutical sciences, 2001. **13**(2): 123-133.

36. Gouda, R., Baishya H. and Qing Z., *Application of mathematical models in drug release kinetics of carbidopa and levodopa ER tablets.* J. Dev. Drugs, 2017. **6**(02): 1-8.